European Journal of Medicinal Chemistry 218 (2021) 113360

Contents lists available at ScienceDirect

European Journal of Medicinal Chemistry

journal homepage: http://www.elsevier.com/locate/ejmech

Identification of *N*-phenyl-2-(phenylsulfonyl)acetamides/propanamides as new SLC-0111 analogues: Synthesis and evaluation of the carbonic anhydrase inhibitory activities

Mostafa M. Elbadawi [a, b], Wagdy M. Eldehna [a, *], Alessio Nocentini [c, d], Mahmoud F. Abo-Ashour [e], Eslam B. Elkaeed [f, g], Mohamed A. Abdelgawad [h], Khalid S. Alharbi [i], Hatem A. Abdel-Aziz [j], Claudiu T. Supuran [c, **], Paola Gratteri [d], Mohammad M. Al-Sanea [h]

[a] Department of Pharmaceutical Chemistry, Faculty of Pharmacy, Kafrelsheikh University, Kafrelsheikh 33516, Egypt
[b] Department of Chemistry, Graduate School of Science, Hiroshima University, 1-3-1 Kagamiyama, Higashi-Hiroshima, Hiroshima 739-8526, Japan
[c] Department of NEUROFARBA, Section of Pharmaceutical and Nutraceutical Sciences, University of Florence, Polo Scientifico, Via U. Schiff 6, 50019, Sesto Fiorentino, Firenze, Italy
[d] Department of NEUROFARBA, Section of Pharmaceutical and Nutraceutical Sciences, Laboratory of Molecular Modeling Cheminformatics & QSAR, University of Florence, Polo Scientifico, Via U. Schiff 6, 50019, Sesto Fiorentino, Firenze, Italy
[e] Department of Pharmaceutical Chemistry, Faculty of Pharmacy, Egyptian Russian University, Badr City, Cairo 11829, Egypt
[f] Department of Pharmaceutical Sciences, College of Pharmacy, AlMaarefa University, Ad Diriyah 13713, Riyadh, Saudi Arabia
[g] Department of Pharmaceutical Organic Chemistry, Faculty of Pharmacy (Boys), Al-Azhar University, Nasr City 11884, Cairo, Egypt
[h] Department of Pharmaceutical Chemistry, College of Pharmacy, Jouf University, Sakaka, Aljouf 72341, Saudi Arabia
[i] Department of Pharmacology, College of Pharmacy, Jouf University, Sakakah, 72341, Saudi Arabia
[j] Department of Applied Organic Chemistry, National Research Center, Dokki, Cairo 12622, Egypt

ARTICLE INFO

Article history:
Received 18 December 2020
Received in revised form
3 March 2021
Accepted 3 March 2021
Available online 13 March 2021

Keywords:
Carbonic anhydrase inhibitors
Sulfones
Benzenesulfonamide
SLC-0111 analogues
Carboxylic acids
Tail approach

ABSTRACT

As a front-runner selective CA IX inhibitor currently in Phase Ib/II clinical trials, SLC-0111 has been herein exploited as a lead molecule for development of new different sets of *N*-phenyl-2-(phenylsulfonyl) acetamides/propanamides incorporating different functionalities; primary sulfonamide (**5a-f**), free carboxylic (**8a**, **8d**), ethyl ester (**8b**, **8e**), acetyl (**8c**, **8f**) and nitro (**10a**, **10b**), as potential carbonic anhydrase (CA, EC 4.2.1.1) inhibitors. All the prepared analogues have been examined for their CA inhibitory activities towards four human (*h*) isoenzymes, *h*CA I, II, IX and XII. Interestingly, replacement of SLC-0111 ureido linker with the flexible sulfonyl acetamide linker, as well as linker branching and elongation strategies successfully enhanced the inhibitory action toward *h*CA IX isoform, such as in sulfones **5a-d** and **5f** which displayed better activity than SLC-0111. Furthermore, sulfonamide-based sulfone (**5f**) and carboxylic acid-based sulfones (**8a** and **8d**) demonstrated interesting selectivity toward the tumor-related *h*CA IX isoform over both *h*CA I and *h*CA II, which suggests them as promising candidates for further development as potential anticancer candidates. Thereafter, the anti-proliferative action for sulfones **5f**, **8a** and **8d** was examined against breast (MCF-7) and colon (HCT-116) cancer cell lines. Also, sulfone **5f** was further assessed for its impact on the cell cycle progression and apoptosis in HCT-116 cells.

1. Introduction

Carbonic anhydrases (CAs, EC 4.2.1.1) are prevalent and ubiquitous metalloenzymes in all life kingdoms and catalyze a simple but crucial physiological reaction, the conversion of CO_2 and water into bicarbonate and proton [1]. This CA-catalyzed reaction is crucial in various physiological and pathological processes, such as several metabolic reactions (like lipogenesis, ureagenesis and

* Corresponding author.
** Corresponding author.
E-mail addresses: wagdy2000@gmail.com (W.M. Eldehna), claudiu.supuran@unifi.it (C.T. Supuran).

https://doi.org/10.1016/j.ejmech.2021.113360
0223-5234/

gluconeogenesis), pH and CO_2 homeostasis, electrolyte secretion, bone resorption, tumorigenicity and respiration, to name a few [2]. So far, eight evolutionarily unrelated gene CA families have been characterized: α-, β-, γ-, δ-, ζ-, η-, θ- and ι-CAs. The α-CAs are present in vertebrates, bacteria, algae, protozoa, corals, and the cytoplasm of green plants [3].

Regarding the human α-CAs (*h*CAs), fifteen assorted isoforms have been identified to date, all of them are catalytically active except CA VIII, X, and XI that are completely lacking the catalytic activity which is attributable to the absence of the essential histidine residues that involved in the catalytic mechanism *via* coordinating the zinc ion [3]. The twelve catalytically active *h*CAs possessed various tissue distribution and location: IV, IX, XII, and XIV are membrane-associated; I, II, III, VII, and XIII are cytosolic; VA and VB are mitochondrial; and VI is secreted in saliva and milk. Inhibition of many of these *h*CA isoforms was demonstrated to provide substantial druggable therapeutic effects for different disorders such as edema (*h*CA II, IV, XIV), glaucoma (*h*CA II, IV and XII), CNS-associated pathologies (*h*CA VII and XIV), and cancers (*h*CA IX and *h*CA XII) [4].

Due to its overexpression in a range of human malignancies, *h*CA IX has been validated as a promising new target in anticancer drug discovery and development for the management of hypoxic tumors [5]. One of the important issues to be considered in the design of *h*CA IX inhibitors is their selectivity over the physiologically relevant cytosolic *h*CA I and II isoforms. In spite of identifying several approaches that develop selective *h*CA IX inhibitors, the "tail approach" emerged as the most exploited and successful one [6]. In this approach, "tails" with a varied chemical nature, are appended to an aromatic/heterocyclic ring featuring a zinc binding group (ZBG), such as primary sulfamoyl and carboxylic acid functionalities, through a flexible linker.

SLC-0111, a front-runner small molecule CAI, is currently in Phase I/II clinical trials for the treatment of metastatic solid hypoxic tumors. As it entails the "tail approach" design, SLC-0111 has high selectivity toward *h*CA IX isoform over the physiologically relevant *h*CA I and II isoforms [7,8]. Furthermore, a recent study [9] has revealed that utilization of SLC-0111 in a combination therapy with 3-*O*-acetylbetulin has efficiently improved the cytotoxicity, enhanced DNA damage, inhibited the cell motility, and enhanced the radiosensitivity. Thence, this study [9] has suggested SLC-0111-based combination therapy as a promising therapeutic approach for targeting different hypoxic tumors.

With the prime aim of identifying new different SLC-0111 analogues, the bioisosteric replacement approach was ultimately fostered by many research groups: the SLC-0111 ureido linker has been replaced with a thioureido and selenoureido (Compound **I**, Fig. 1) [10], 1,3-triazene (Compound **II**, Fig. 1) [11], cyanoguanidine (Compound **III**, Fig. 1) [12], enaminone (Compound **IV**, Fig. 1) [13], and rigid piperazinyl-ureido linkers (Compound **V**, Fig. 1) [14]. Though most these reported SLC-0111 analogues elicited an enhanced *h*CA IX inhibitory activity, their inhibition profiles exhibited loss of selectivity toward *h*CA IX over the cytosolic *h*CA II isozyme, which should be attributable to the concurrent considerable improvement of *h*CA II inhibitory activity.

Herein we report the design and synthesis of new SLC-0111 analogues based on *N*-phenyl-2-(phenylsulfonyl)acetamide/propanamide scaffold that incorporates different functionalities; primary sulfonamide (**5a-f**), free carboxylic acid (**8a** and **8d**), ethyl ester (**8b** and **8e**), acetyl (**8c** and **8f**) and nitro (**10a-b**), as (Fig. 2). The utilized design strategy is based on replacement of the SLC-0111 ureido linker with the flexible sulfonyl acetamide linker. Thereafter, the sulfonyl acetamide linker was either branched or elongated. Moreover, a bioisosteric replacement for the sulfamoyl zinc-binding group with carboxylic acid functionality as well as ethyl ester, acetyl and nitro groups, was carried out. All the newly prepared *N*-phenyl-2-(phenylsulfonyl)acetamides/propanamides **5a-f**, **8a-f** and **10a-b** will be characterized and biologically evaluated towards a panel of *h*CA I, II, IX and XII isoforms.

2. Results and discussion

2.1. Chemistry

The synthetic routes followed to synthesize the differently substituted *N*-phenyl-2-(phenylsulfonyl)acetamides/propanamides (**5a-f**, **8a-f** and **10a-b**) are depicted in Schemes 1 and 2.

In Scheme 1, synthesis of the target benzenesulfonamide-containing derivatives (**5a-f**) was started by acylation of the basic amino function of sulfanilamide **1** with bromoacetyl bromide **2a**, 2-bromopropionyl bromide **2b**, or 3-chloropropionyl chloride **2c** in dry dioxane in the presence of potassium carbonate to afford the key intermediates **3a-c**, respectively. Then, intermediates **3a-c** were reacted with sodium sulfinates **4a,b** in absolute ethanol to afford the target benzenesulfonamide-based sulfones **5a-f** (Scheme 1).

With the aim of introducing different isosteres for the sulfonamide functionality, four different aniline derivatives **6a-d** (4-aminobenzoic acid, ethyl 4-aminobenzoate, 4-aminoacetophenone and 4-nitroaniline) were acylated by bromoacetyl bromide **2a** as described above to afford intermediates **7a-c** and **9**, respectively. Thereafter, intermediates **7a-c** and **9** were reacted with sodium sulfinates **4a,b** in absolute ethanol to furnish the target sulfones **8a-f** and **10a-b**, respectively (Scheme 2).

All herein prepared target sulfones **5a-f**, **8a-f** and **10a-b** were obtained in good yields and thoroughly characterized by ^{1}H NMR, ^{13}C NMR and HRMS.

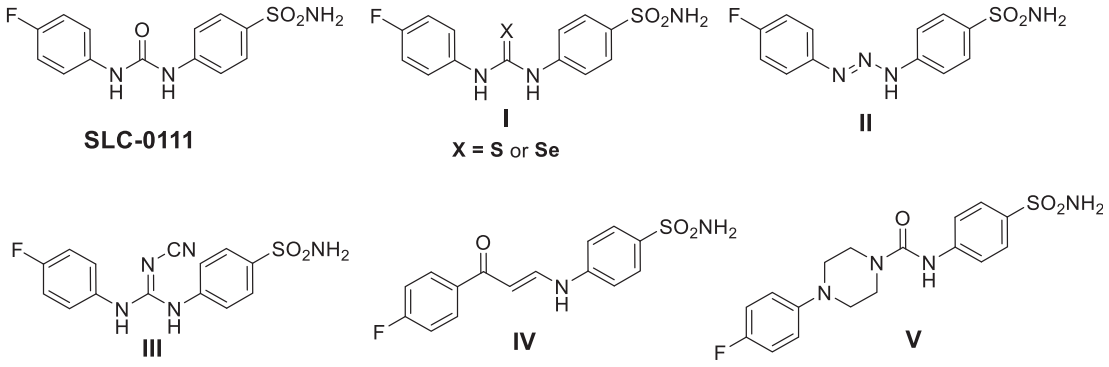

Fig. 1. Structure of SLC-0111 and its analogues **I**–**V**.

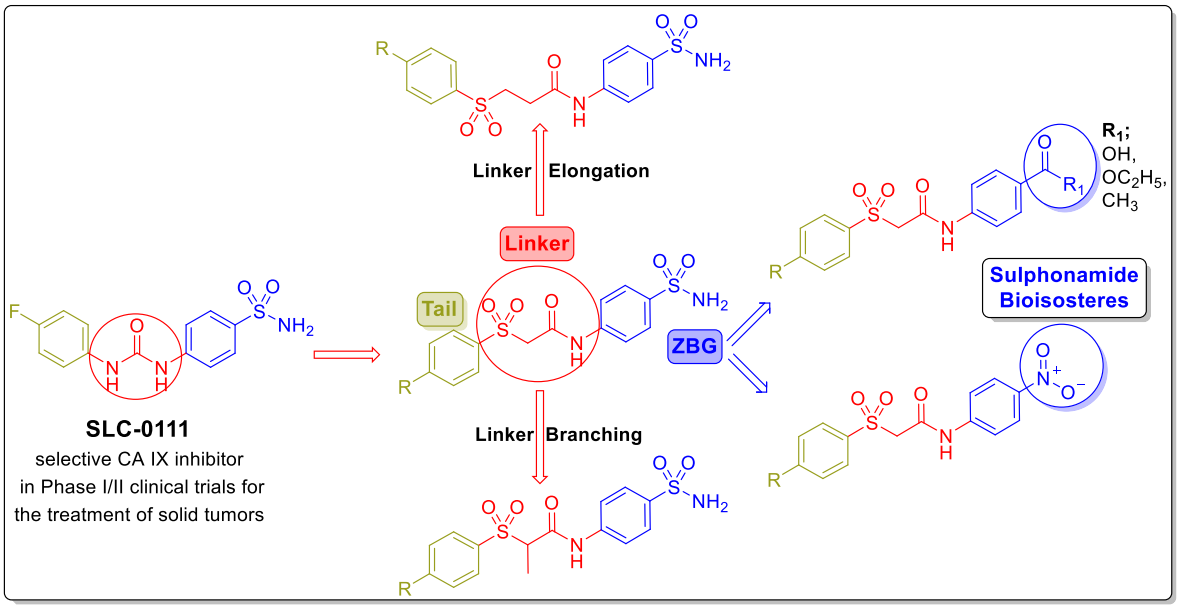

Fig. 2. The design for the target *N*-phenyl-2-(phenylsulfonyl)acetamides/propanamides **5a-f**, **8a-f** and **10a**, **b**.

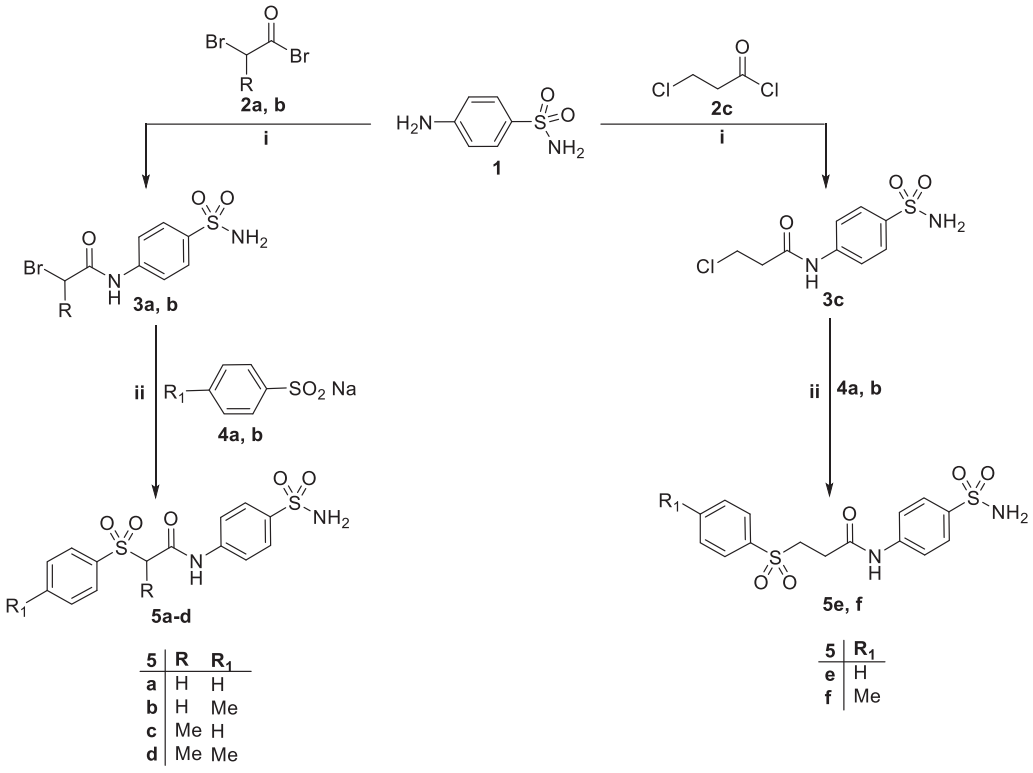

5	R	R1
a	H	H
b	H	Me
c	Me	H
d	Me	Me

5	R1
e	H
f	Me

Scheme 1. Synthesis of target sulfonamides **5a-f**; *Reagents and conditions*: (**i**) Dioxane, K_2CO_3, stirring 3 h, (**ii**) Ethanol/reflux 14 h.

2.2. Carbonic anhydrase inhibition

The CA inhibitory impact for all herein prepared target sulfones **5a-f**, **8a-f** and **10a-b**, as well as the standard CAI acetazolamide (**AAZ**) was estimated against the ubiquitous cytosolic CA I and II, and cancer-related CA IX and XII isoforms, by the use of a stopped-flow CO_2 hydrase assay [15]. Certain structure–activity relationship (SAR) could be collected from the reported inhibition data in Tables 1 and 2.

Regarding the CA inhibitory activities of sulfonamide-based *N*-phenyl-2-(phenylsulfonyl)acetamides/propanamides (**5a-f**), all derivatives displayed potent to moderate inhibitory action towards the ubiquitous cytosolic *h*CA I isoform with K_I values ranging from 72.1 to 320.4 nM, Table 1. In particular, sulfonamide-based sulfones **5b**, **5c** and **5d** exhibited the best *h*CA I inhibitory activity with two-digit nanomolar activities (K_Is = 72.1, 92.6 and 83.8 nM,

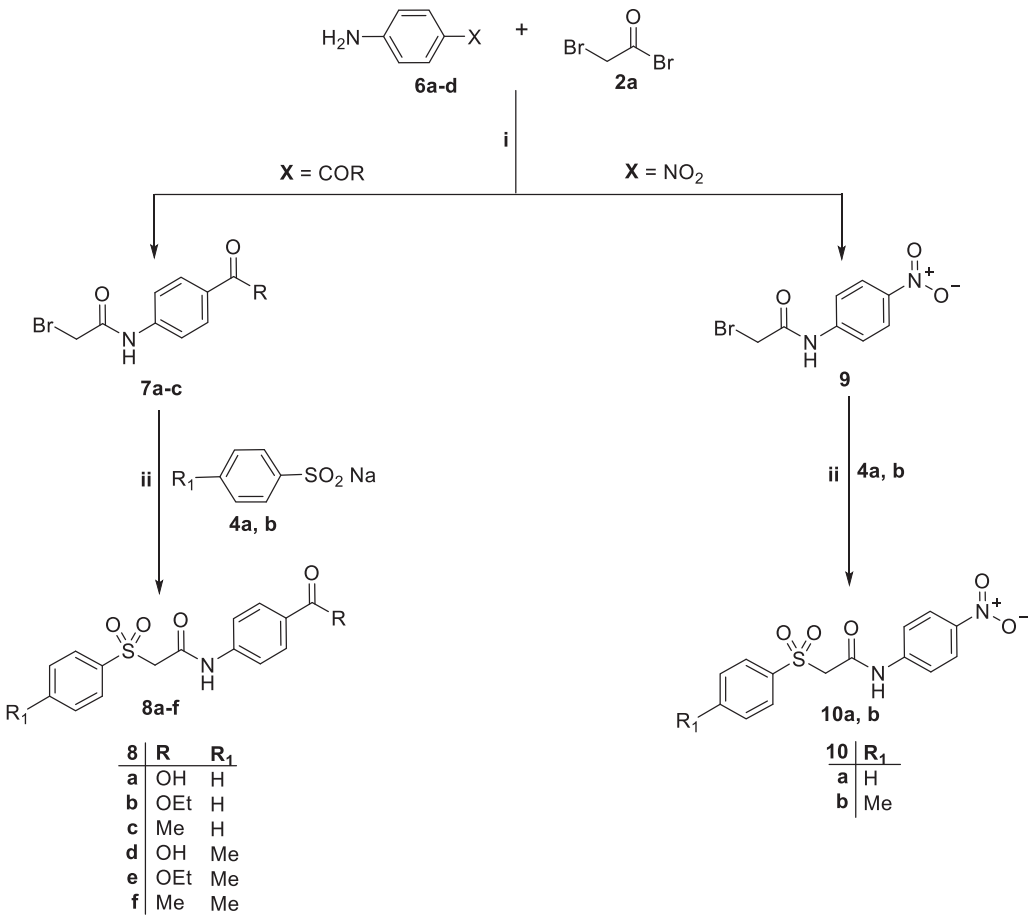

8	R	R_1
a	OH	H
b	OEt	H
c	Me	H
d	OH	Me
e	OEt	Me
f	Me	Me

10	R_1
a	H
b	Me

Scheme 2. Synthesis of target sulfones **8a-f** and **10a, b**; *Reagents and conditions*: (**i**) Dioxane, K_2CO_3, stirring 3 h, (**ii**) Ethanol/reflux 10 h.

respectively), whereas sulfones **5a**, **5e** and **5f** exerted moderate activity with K_Is equal 320.4, 114.2 and 129.7 nM, respectively. It is worth stressing that grafting a *p*-methyl group (compound **5b**; K_I = 72.1 nM) within the phenyl tail of sulfone **5a** (K_I = 320.4 nM) resulted in a more than 4-fold inhibition increase for the cytosolic *h*CA I isoform. Also, it is noted that branching and elongation of the sulfonyl acetamide linker in the phenyl tail-bearing sulfone **5a** (K_I = 320.4 nM) resulted in a slight enhancement of isoform *h*CA I inhibitory activity (compounds **5c** and **5e**; K_Is = 92.6 and 114.2 nM, respectively). On the other hand, branching and elongation of the sulfonyl acetamide linker in the *p*-tolyl tail-bearing sulfone **5b** (K_I = 72.1 nM) led to sulfones **5d** and **5f** with slight decreased activity against *h*CA I isoform (K_Is = 83.8 and 129.7 nM, respectively).

Furthermore, exploring the inhibitory activity of herein reported sulfonamide-based sulfones (**5a-f**) against the physiologically dominant *h*CA II isoform revealed that it was effectively inhibited by sulfones (**5a-f**) with K_I spanning in the range 5.9–43.6 nM, Table 1. Superiorly, sulfones **5c** and **5d** exerted single-digit nanomolar inhibitory activities against *h*CA II isoform (K_Is = 7.4 and 5.9 nM, respectively), in addition sulfones **5a**, **5b**, **5e** and **5f** displayed inhibition constants equal 43.6, 14.7, 31.8 and 20.3 nM, respectively. It is worthy to mention that replacement of the phenyl tail of sulfone **5a** (K_I = 43.6 nM) with a *p*-tolyl one, as in compound **5b**, resulted in about 3-fold enhanced inhibitory potency toward *h*CA II isoform (K_I = 14.7 nM). Moreover, branching of the sulfonyl acetamide linker as well as its elongation improved the *h*CA II inhibitory action for the phenyl tail-bearing sulfone **5a**; (compounds **5c** and **5e**; K_Is = 7.4 and 31.8 nM, respectively).

The obtained inhibition constants for the tumor-related isoform *h*CA IX (Table 1), showed that all sulfonamide-based sulfones (**5a-f**) were capable of inhibiting this isoform in the low nanomolar range (K_Is: 4.3–46.1 nM). Sulfones **5c** and **5f** emerged as the most potent herein reported *h*CA IX inhibitors endowed with single-digit nanomolar K_I values equal 6.5 and 4.3 nM, respectively, Table 1. Similar to the SAR for inhibition of *h*CA I and II; grafting a *p*-methyl group (compound **5b**; K_I = 15.9 nM) within the phenyl tail of sulfone **5a** (K_I = 22.7 nM) was advantageous for inhibitory activity against *h*CA IX. Also, branching of the sulfonyl acetamide linker incorporated in the phenyl tail-bearing sulfone **5a** was more beneficial for *h*CA IX inhibition (compound **5c**; K_I = 6.5 nM), whereas, elongation of such linker resulted in about 2-fold decreased activity towards *h*CA IX isoform (compound **5e**; K_I = 46.1 nM). On the contrary, elongation of the sulfonyl acetamide linker in the *p*-tolyl tail-bearing sulfone **5b** (K_I = 15.9 nM) to a sulfonyl propanamide linker led to the most efficient *h*CA IX inhibitor (**5f**) with K_I = 4.3 nM, whereas linker branching for sulfone **5b** decreased the activity approximately by half (K_I = 29.8 nM), Table 1.

Finally, the displayed *in vitro* inhibition data (Table 1) highlighted that the cancer-related *h*CA XII isoform has been effectively inhibited by all the sulfonamide-bearing sulfones (**5a-f**) herein reported. The *h*CA XII inhibition profiles were almost flat, with measured K_I values ranged from 5.1 to 42.4 nM. The SAR outcomes pointed out that incorporation of a branched sulfonyl propanamide linker led to sulfones **5c** and **5d** which stood out as most efficient *h*CA XII inhibitors in this work with single-digit nanomolar

Table 1
Inhibition data for *h*CA I, II, IX and XII isoforms with sulfonamide-based *N*-phenyl-2-(phenylsulfonyl)acetamides/propanamides (**5a-f**), SLC-0111, and the standard **AAZ**.

Code	Structure	K_I (nM)[a]			
		CA I	CA II	CA IX	CA XII
5a	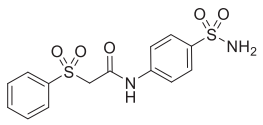	320.4	43.6	22.7	11.2
5b	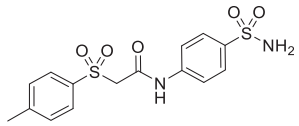	72.1	14.7	15.9	42.4
5c	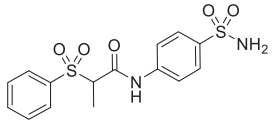	92.6	7.4	6.5	5.1
5d	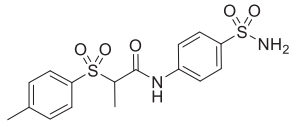	83.8	5.9	29.8	7.9
5e	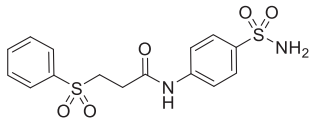	114.2	31.8	46.1	32.6
5f	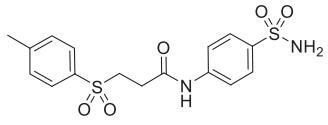	129.7	20.3	4.3	35.8
SLC-0111		5080	960.0	45.0	4.5
AAZ		250.0	12.0	25.0	5.7

a; Mean from three different assays, *via* a stopped flow technique.

inhibitory potencies (K_Is = 5.1 and 7.9 nM, respectively), Table 1.

With regard to the newly synthesized non-sulfonamide-based *N*-phenyl-2-(phenylsulfonyl)acetamides (**8a-f** and **10a-b**), their *h*CA inhibitory activities were assessed and the obtained inhibition data were listed in Table 2.

Bioisosteric replacement of the sulfamoyl zinc-binding group in sulfones **5a** and **5b** with the carboxylic acid functionality (sulfones **8a** and **8d**) dramatically affected the inhibitory activities. Both carboxylic acid-based sulfones **8a** and **8d** displayed diminished or weak inhibition against *h*CA I (K_Is = >100 and 55.7 μM, respectively) and *h*CA II (K_Is = 31.7 and 15.8 μM, respectively) isoforms, whereas they displayed moderate sub-micromolar inhibitory potencies against *h*CA IX (K_Is = 0.93 and 0.72 μM, respectively) and *h*CA XII (K_Is = 0.85 and 0.53 μM, respectively) isoforms, Table 2.

Furthermore, ester analogues (**8b** and **8e**) of carboxylic acid-based sulfones **8a** and **8d** displayed much lower inhibitory activities towards the examined *h*CA I (K_Is = >100 μM), II (K_Is = >100 and 91.4 μM, respectively), IX (K_Is = 17.2 and 29.5 μM, respectively), and XII (K_Is = 1.4 and > 100 μM, respectively) isoforms, Table 2.

On the other hand, replacement of the primary sulfonamide functionality in sulfones **5a** and **5b** with acetyl (sulfones **8c** and **8f**) or nitro (sulfones **10a** and **10b**) functionalities diminished the inhibitory activities toward all the examined *h*CA isoforms I, II, IX and XII (K_Is > 100 μM), Table 2.

It is worth highlighting that carbonic anhydrase inhibitory profiles presented in Tables 1 and 2 hinted out that only

Table 2
Inhibition data for *h*CA isoforms I, II, IX and XII with non-sulfonamide-based *N*-phenyl-2-(phenylsulfonyl)acetamides **8a-f** and **10a-b**.

Code	Structure	K_I (μM)			
		CA I	CA II	CA IX	CA XII
8a	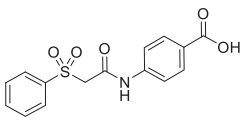	>100	31.7	0.93	0.85
8b	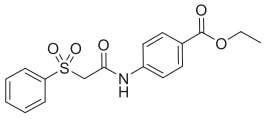	>100	>100	17.2	1.4
8c	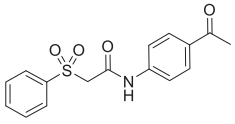	>100	>100	>100	>100
8d	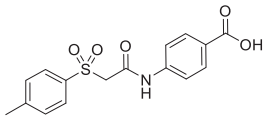	55.7	15.8	0.72	0.53
8e	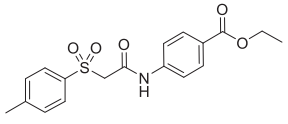	>100	91.4	29.5	>100
8f	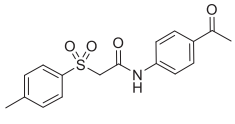	>100	>100	>100	>100
10a	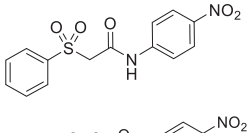	>100	>100	>100	>100
10b	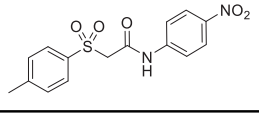	>100	>100	>100	>100

sulfonamide-based sulfone (**5f**) and carboxylic acid-based sulfones (**8a** and **8d**) demonstrated interesting selectivity toward the tumor-related *h*CA IX isoform over both *h*CA I (*S.I.* = 30.2, >107 and 77.4, respectively) and *h*CA II (*S.I.* = 4.7, 34.1 and 21.9, respectively), Table 3. This selectivity manner for sulfones **5f**, **8a** and **8d** suggests them as interesting and promising candidates for further development as potential anticancer agents.

Lastly, the herein utilized bioisosteric replacement approach *via* replacing the SLC-0111 ureido linker with the flexible sulfonyl acetamide linker, as well as linker branching and elongation strategies successfully enhanced the inhibitory action toward *h*CA IX isoform, such as sulfones **5a-d** and **5f** (K_Is = 22.7, 11.2, 6.5, 5.1 and 32.6 nM, respectively, *vs* K_I = 45.0 for SLC-0111). Regrettably, the enhanced activity toward *h*CA IX was accompanied with an improved activity against *h*CA II isoform, as well, which led to a decreased *h*CA IX/II selectivity index for target sulfones. Thus, further structural modifications are required to optimize the *h*CA IX/II selectivity.

Table 3
Calculated selectivity indexes (*S.I.s*) for inhibition of *h*CA IX over *h*CA I and II isoforms for sulfonamide-bearing sulfone (**5f**), carboxylic acid-based sulfones (**8a** and **8d**), and acetazolamide.

Compound	I/IX	II/IX
5f	30.2	4.7
8a	>107	34.1
8d	77.4	21.9
AAZ	10.0	0.5

2.3. Anticancer study

2.3.1. Anti-proliferative activity against HCT-116 and breast MCF-7 cell lines

On account of their favorable selectivity profile towards *h*CA IX, sulfones **5f**, **8a** and **8d** were selected to be assessed for their potential anti-proliferative action against human colorectal (HCT-116) and breast (MCF-7) cancer cell lines, under hypoxic conditions utilizing the protocol of the MTT assay. The assay results have been expressed as IC_{50} values and listed in Table 4.

Investigating the MTT assay results highlighted that the tested sulfones **5f**, **8a** and **8d** possessed excellent to moderate growth inhibitory activity against both HCT-116 and MCF-7 cell lines. Interestingly sulfonamide-based sulfone **5f**, which displayed potent *h*CA IX inhibitory activity, showed excellent sub-micromolar anti-proliferative activity against HCT-116 ($IC_{50} = 0.57 \pm 0.02$) and MCF-7 cells ($IC_{50} = 0.67 \pm 0.03$). Moreover, non-sulfonamide-based sulfones **8a** and **8d** exhibited moderate activity against HCT-116 ($IC_{50} = 11.58 \pm 0.44$ and 2.23 ± 0.08, respectively) and MCF-7 ($IC_{50} = 5.29 \pm 0.2$ and 3.41 ± 0.13, respectively) cells, Table 4.

2.3.2. Cell cycle analysis

The impact of sulfonamide-based sulfone **5f** on the cell cycle progression in colorectal HCT-116 cells was explored *via* a flow cytometric analysis.

Analyzing the obtained results hinted out that exposure of HCT-116 cells to sulfone **5f** for 24 h affected the cell cycle progression. Sulfone **5f** was found to increase the percentage of apoptotic cells within Sub-G_1 phase, in addition to the cell populations in the S-phase. Moreover, **5f** decreased the G_2-M phase populations by 3-fold compared to the control, Fig. 3.

2.3.3. Annexin V-FITC/Propidium Iodide (AV/PI) apoptosis assay

The potential apoptotic effect of sulfone **5f** in colorectal HCT-116 cells was examined, utilizing (AV/PI) dual staining assay. The assay outputs highlighted the ability of sulfone **5f** to persuade apoptosis in HCT-116 cells as suggested by the significant increase in the percent of AV-positive apoptotic cells in the late apoptosis phase from 0.22% to 21.45% (Fig. 4).

2.4. Docking study

A docking study was implemented to estimate the correlation between ligand structure and inhibition potency against *h*CAs II, IX and XII. Sulfonamide-based sulfones **5a** and **5e** were chosen as representative of the sulfonamide subset, and **8a** as exemplary carboxylate.

All docking solutions found the benzenesulfonamide moiety of sulfones **5a** and **5e** coordinated to the zinc ion by the negatively charged nitrogen atom according to a tetracoordinated geometry. Furthermore, the poses were stabilized by two H-bonds established by the sulfonamide S=O and NH^- groups with the NH backbone and OH side chain of residues T199, respectively. The phenyl ring formed hydrophobic contacts with nonpolar residues V121, V143 and L198 (Fig. 5).

The phenylsulfonyl tail of the two ligands, which only differ in length for a −CH2- group, accommodated over the hydrophobic area of the active site of *h*CAs II, IX and XII. This area, lined by the residue 91, 121, 131, 135, 141, 143, 198, 201, 202, 204, shows in *h*CA II the most lipophilic properties and the smallest volume among this *h*CA subset due to the presence of the F131 residue that is replaced by valine/XX in the CA IX/XII isoforms. This enables an efficient fit of the ligand tails within this area, further stabilized by π and hydrophobic interactions (Fig. 5A). These ligand orientations appear to tolerate a *p*-methylation on the outer phenyl ring, as in **5b**, **5d** or **5f** that increased the inhibition potency.

Equally lipophilic, in *h*CA IX the same area displays a greater volume because of the F131V mutation with respect to *h*CA II. Thus, the phenylsulfonyl tail is able to stretch inside the cleft forming a wide set of π-alkyl and hydrophobic interactions (Fig. 5B). These orientations also appear to tolerate the *p*-methylation, as in **5b**, or **5f**, that in fact increased the compound inhibition potency. The lipophilic features of the same area in *h*CA XII is significantly reduced because of the L204 N, V135 and G132S mutations with respect to hCA II. The phenylsulfonyl group of the ligand is involved in a wide network of VdW interactions with S132, S136, N136, P202 and N204 which together efficiently stabilize the binding orientations (Fig. 5C). However, the nature of the pocket did not tolerate the ligand *p*-methylation and induced, in the case of hCA XII a slight decrease of inhibition potency for the toluyl derivatives **5b** and **5f**.

Carboxylates are generally much less efficient than primary sulfonamides as zinc-binders for CA inhibition [2]. Likewise, carboxylates **8a**, **8b**, **8d**, and **8e** acted as significantly worse CAIs than sulfonamides **5a-f** (Table 2). The docking solutions for the carboxylic acid **8a** showed the COO^- group coordinating the zinc ion by a tetrahedral geometry in the active site of *h*CA II, IX and XII. The orientation of **8a** zinc-binding function was significantly stabilized by a H-bond with T199 backbone NH in the active site of *h*CAs IX and XII (Fig. 6). The presence of F131 was shown to narrow *h*CA II active site enough to hinder the aforesaid positioning and stabilization for the benzoate portion, that overall decreased the

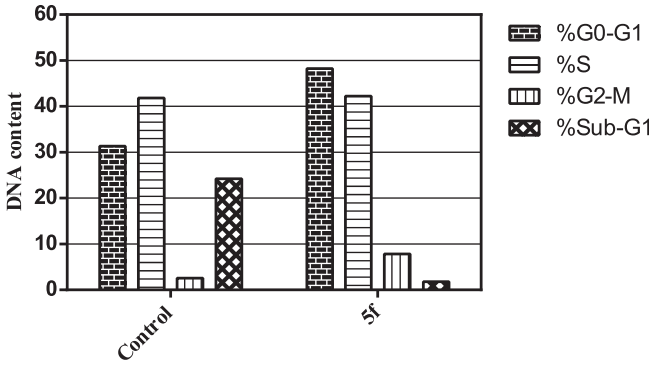

Fig. 3. Effect of sulfonamide-based sulfone **5f** on the cell cycle phases in HCT-116 cells.

Table 4
Anti-proliferative impact of sulfones **5f**, **8a** and **8d** against human colorectal (HCT-116) and breast (MCF-7) cancer cell lines, under hypoxic conditions.

Comp.	IC_{50} (μM)[a]	
	HCT-116	MCF-7
5f	0.57 ± 0.02	0.67 ± 0.03
8a	11.58 ± 0.44	5.29 ± 0.2
8d	2.23 ± 0.08	3.41 ± 0.13

[a] IC_{50} values are the mean ± S.D. of three experiments.

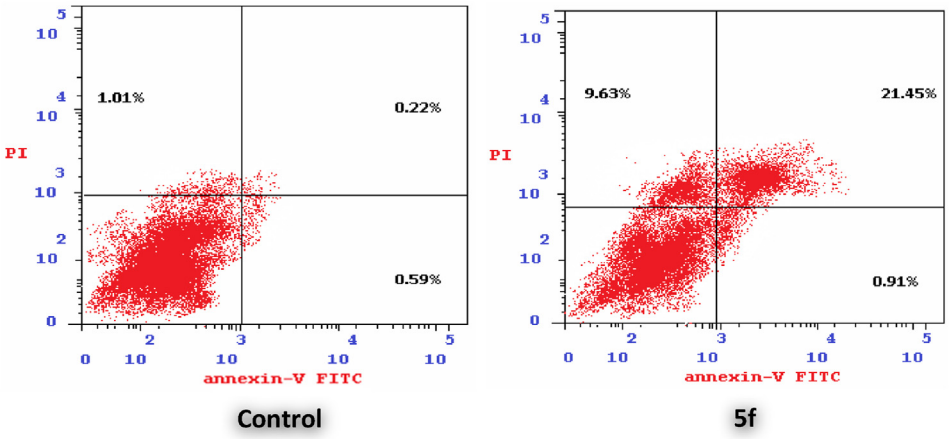

Fig. 4. Effect of sulfonamide-based sulfone **5f** on the percentage of AV-positive staining in in colorectal HCT-116 cells.

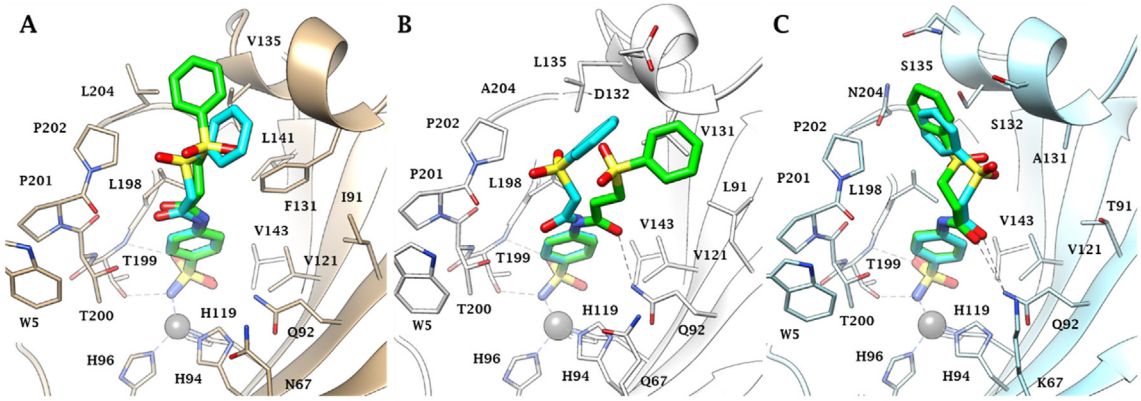

Fig. 5. Predicted binding orientations of sulfonamide-based sulfones **5a** (cyan) and **5e** (green) within the active site of **A**) *h*CA II, **B**) *h*CA IX and **C**) *h*CA XII. H-bonds are represented as black dashed lines.

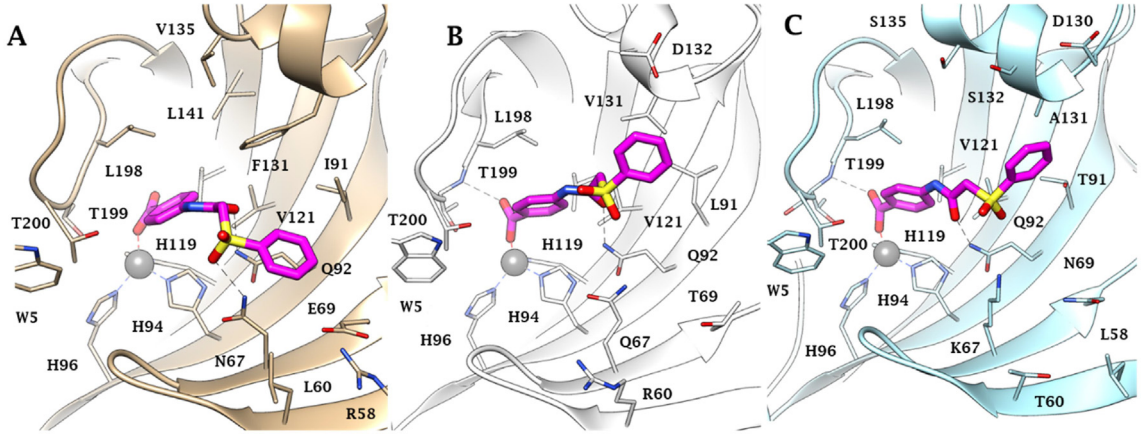

Fig. 6. Predicted binding orientations of carboxylic acid **8a** within the active site of **A**) *h*CA II, **B**) *h*CA IX and **C**) *h*CA XII. H-bonds are represented as black dashed lines.

inhibition potency against *h*CA II with respect to *h*CAs IX and XII (Table 2). As a result of the different positioning of the benzoate core, the ligand tail protruded towards the pocket lined by residues 91, 92, and 131 in the active site of the tumor-associated CAs, accommodating over the area formed by Q92, E69, N67 and L60 in *h*CA II binding cleft. In all the three active site ligand amidic carbonyl group received a H-bond by Q92 side chain NH_2 (Fig. 6).

3. Conclusion

In this work, novel *N*-phenyl-2-(phenylsulfonyl)acetamides/propanamides incorporating primary sulfonamide (**5a-f**), free carboxylic (**8a**, **8d**), ethyl ester (**8b**, **8e**), acetyl (**8c**, **8f**) and nitro (**10a**, **10b**) functionalities have been designed and prepared as novel SLC-0111 analogues. Sulfonamide-based sulfones **5** displayed much

better activity than their carboxylic acids and esters analogues, whereas acetyl and nitro counterparts showed diminished CA inhibitory activities. Sulfonamide-based sulfones **5** displayed K_Is in the nanomolar range; 72.1–320.4 nM for CA I, 5.9–43.6 nM for CA II, 4.3–46.1 nM for CA XI, and 5.1–42.4 nM for CA XII. The SAR analysis pointed out that replacement of the phenyl tail with a *p*-tolyl one, as well as branching of the sulfonyl acetamide linker are more advantageous for the inhibitory activities towards *h*CA I, II and IX isoforms. Superiorly, sulfones **5c** and **5f** emerged as the most potent herein reported *h*CA IX inhibitors with single-digit nanomolar potency (K_I = 6.5 and 4.3 nM, respectively), whereas sulfones **5c** and **5d** stood out as most efficient single-digit nanomolar *h*CA XII inhibitors in this study with K_Is = 5.1 and 7.9 nM, respectively. Furthermore, sulfonamide-based sulfone (**5f**) and carboxylic acid-based sulfones (**8a** and **8d**) demonstrated interesting selectivity toward the tumor-related *h*CA IX isoform over both *h*CA I (*S.I.* = 30.2, >107 and 77.4, respectively) and *h*CA II (*S.I.* = 4.7, 34.1 and 21.9, respectively), which suggested them for further biological evaluation as potential anticancer agents. The anti-proliferative action for sulfones **5f**, **8a** and **8d** was then examined against breast (MCF-7) and colon (HCT-116) cancer cell lines. Moreover, sulfone **5f** was further assessed for its action on the cell cycle distribution and apoptosis in HCT-116 cells. Finally, the molecular docking study has justified the obtained CA inhibitory activities, and has explored the binding mode for the target sulfones within *h*CA II, IX and XII active sites.

4. Experimental

4.1. Chemistry

4.1.1. General

The NMR spectra have been recorded on Bruker spectrophotometer at 400 MHz. ^{13}C spectra were run at 100 MHz in deuterated dimethyl sulfoxide (DMSO-d_6). Chemical shifts (δ_H) are reported relative to TMS as internal standard. High-resolution mass spectra have been recorded on Bruker MicroTOF spectrometer. Compounds **3a-c** [16–19], **7a-c** [20–22] and **9** [23] were previously synthesized.

4.1.2. General procedure for preparation of target N-phenyl-2-(phenylsulfonyl) acetamides/propanamides 5a-f, 8a-f and 10a-b

To a hot stirred solution of 2-bromo-*N*-phenylacetamides (**3a-b**, **7a-c** and **9**) and 3-chloro-*N*-(4-sulfamoylphenyl)propanamide (**3c**) intermediates (0.5 mmol) in absolute ethanol (15 mL), sodium sulfinates **4a,b** (0.65 mmol) were added. The reaction mixture was then heated under reflux for 14 h (for sulfonamides **5a-f**) or 10 h (for sulfones **8a-f** and **10a-b**). After the completion of the reaction, the reaction mixture was evaporated under reduced pressure, and then cold water (20 mL) was added to the residue. The remaining solid was filtered-off, dried, and crystalized from acetonitrile to produce the target sulfones (**5a-f**, **8a-f** and **10a-b**) in 68–85% yield.

4.1.2.1. 2-(Phenylsulfonyl)-N-(4-sulfamoylphenyl)acetamide 5a. White crystals, m.p. 213–215 °C, yield 72%, ^{1}H NMR (400 MHz) *δ ppm*: 4.52 (s, 2H, -C<u>H</u>$_2$-CO), 7.31 (s, 2H, NH$_2$), 7.59 (d, 2H, Ar–H, *J* = 8.8 Hz), 7.65–7.77 (m, 3H, Ar–H), 7.89 (d, 2H, Ar–H, *J* = 8.4 Hz), 7.91 (d, 2H, Ar–H, *J* = 8.8 Hz), 10.60 (s, 1H, NH); ^{13}C NMR (100 MHz) *δ ppm*: 62.84, 119.10, 126.47, 128.49, 129.75, 130.96, 134.57, 139.81, 142.45, 160.41, 167.07.

4.1.2.2. N-(4-Sulfamoylphenyl)-2-tosylacetamide 5b. White crystals, m.p. 227–228 °C, yield 68%, ^{1}H NMR (400 MHz) *δ ppm*: 2.42 (s, 3H, –C$_6$H$_4$–C<u>H</u>$_3$), 4.47 (s, 2H, -C<u>H</u>$_2$-CO), 7.27 (s, 2H, NH$_2$), 7.45 (d, 2H, Ar–H, *J* = 8.0 Hz), 7.60 (d, 2H, Ar–H, *J* = 8.8 Hz), 7.78 (d, 2H, Ar–H, *J* = 8.4 Hz), 7.90 (d, 2H, Ar–H, *J* = 8.4 Hz), 10.59 (s, 1H, NH); ^{13}C NMR (100 MHz) *δ ppm*: 21.57, 62.76, 119.08, 125.98, 126.48, 128.55, 130.17, 130.95, 136.90, 142.67, 145.13, 160.56, 167.28; HRMS (ESI) for $C_{15}H_{17}O_5N_2S_2$, calcd 369.05734, found 369.05809 [M+H]$^+$.

4.1.2.3. 2-(Phenylsulfonyl)-N-(4-sulfamoylphenyl)propanamide 5c. White crystals, m.p. 196–197 °C, yield 79%, ^{1}H NMR (400 MHz) *δ ppm*: 1.40 (d, 3H, -C<u>H</u>$_3$-CH-CO, *J* = 6.8 Hz), 4.36 (q, 1H, –CH$_3$-C<u>H</u>-CO, *J* = 6.8 Hz), 7.29 (s, 2H, NH$_2$), 7.65–7.68 (m, 4H, Ar–H), 7.76–7.80 (m, 3H, Ar–H), 7.83–7.86 (m, 2H, Ar–H), 10.62 (s, 1H, NH); ^{13}C NMR (100 MHz) *δ ppm*: 12.41, 65.96, 119.57, 127.26, 129.57, 129.71, 134.87, 136.81, 139.73, 141.64, 164.11; HRMS (ESI) for $C_{15}H_{17}O_5N_2S_2$, calcd 369.05734, found 369.05727 [M+H]$^+$.

4.1.2.4. N-(4-Sulfamoylphenyl)-2-tosylpropanamide 5d. White crystals, m.p. 205–206 °C, yield 71%, ^{1}H NMR (400 MHz) *δ ppm*: 1.37 (d, 3H, -C<u>H</u>$_3$-CH-CO, *J* = 7.2 Hz), 2.41 (s, 3H, –C$_6$H$_4$–C<u>H</u>$_3$), 4.33 (q, 1H, –CH$_3$-C<u>H</u>-CO, *J* = 6.8 Hz), 7.29 (s, 2H, NH$_2$), 7.46 (d, 2H, Ar–H, *J* = 8.0 Hz), 7.67 (d, 2H, Ar–H, *J* = 8.8 Hz), 7.71 (d, 2H, Ar–H, *J* = 8.0 Hz), 7.78 (d, 2H, Ar–H, *J* = 8.8 Hz), 10.63 (s, 1H, NH); ^{13}C NMR (100 MHz) *δ ppm*: 12.52, 21.58, 65.98, 119.54, 127.26, 129.61, 130.16, 133.98, 139.63, 141.56, 145.51, 164.12; HRMS (ESI) for $C_{16}H_{19}O_5N_2S_2$, calcd 383.07299, found 383.07305 [M+H]$^+$.

4.1.2.5. 3-(Phenylsulfonyl)-N-(4-sulfamoylphenyl)propanamide 5e. White crystals, m.p. 185–186 °C, yield 75%, ^{1}H NMR (400 MHz) *δ ppm*: 2.71 (t, 2H, –CH$_2$-C<u>H</u>$_2$-CO, *J* = 7.6 Hz), 3.62 (t, 2H, -C<u>H</u>$_2$-CH$_2$-CO, *J* = 7.6 Hz), 7.23–7.29 (m, 3H, Ar–H), 7.64–7.75 (m, 4H, Ar–H), 7.80 (s, 2H, NH$_2$), 7.92–7.99 (m, 2H, Ar–H), 10.77 (s, 1H, NH); ^{13}C NMR (100 MHz) *δ ppm*: 29.96, 51.02, 119.07, 119.79, 127.14, 127.32, 128.25, 129.98, 130.31, 134.45, 135.44, 139.10, 140.54, 142.24, 168.37; HRMS (ESI) for $C_{15}H_{17}O_5N_2S_2$, calcd 369.05734, found 369.05820 [M+H]$^+$.

4.1.2.6. N-(4-Sulfamoylphenyl)-3-tosylpropanamide 5f. White crystals, m.p. 219–221 °C, yield 73%, ^{1}H NMR (400 MHz) *δ ppm*: 2.38 (s, 3H, –C$_6$H$_4$–C<u>H</u>$_3$), 2.69 (t, 2H, –CH$_2$-C<u>H</u>$_2$-CO, *J* = 7.2 Hz), 3.57 (t, 2H, -C<u>H</u>$_2$-CH$_2$-CO, *J* = 7.2 Hz), 7.24 (s, 2H, NH$_2$), 7.44 (d, 2H, Ar–H, *J* = 7.6 Hz), 7.62 (d, 2H, Ar–H, *J* = 8.8 Hz), 7.73 (d, 2H, Ar–H, *J* = 8.8 Hz), 7.78 (d, 2H, Ar–H, *J* = 8.0 Hz), 10.33 (s, 1H, NH); ^{13}C NMR (100 MHz) *δ ppm*: 21.51, 30.24, 51.10, 119.06, 119.67, 127.11, 128.33, 130.39, 134.87, 136.13, 138.87, 142.18, 144.97, 168.47; HRMS (ESI) for $C_{16}H_{19}O_5N_2S_2$, calcd 383.07299, found 383.07307 [M+H]$^+$.

4.1.2.7. 4-(2-(Phenylsulfonyl)acetamido)benzoic acid 8a. White crystals, m.p. 247–249 °C, yield 80%, ^{1}H NMR (400 MHz) *δ ppm*: 4.53 (s, 2H, -C<u>H</u>$_2$-CO), 7.65–7.77 (m, 5H, Ar–H), 7.86 (d, 2H, Ar–H, *J* = 8.8 Hz), 7.91–7.93 (m, 2H, Ar–H), 10.77 (s, 1H, NH), 12.01 (s, 1H, COO<u>H</u>); ^{13}C NMR (100 MHz) *δ ppm*: 62.63, 119.36, 128.52, 129.50, 129.76, 134.37, 134.60, 139.59, 143.10, 160.78, 169.17; HRMS (ESI) for $C_{15}H_{13}O_5NNaS$, calcd 342.04066, found 342.04087 [M+Na]$^+$.

4.1.2.8. Ethyl 4-(2-(phenylsulfonyl)acetamido)benzoate 8b. White crystals, m.p. 171–173 °C, yield 83%, ^{1}H NMR (400 MHz) *δ ppm*: 1.28 (t, 3H, C<u>H</u>$_3$–CH$_2$-, *J* = 7.2 Hz), 4.25 (q, 2H, CH$_3$–C<u>H</u>$_2$-, *J* = 7.2 Hz), 4.54 (s, 2H, -C<u>H</u>$_2$-CONH-), 7.62 (d, 2H, Ar–H, *J* = 8.8 Hz), 7.67 (d, 2H, Ar–H, *J* = 8.0 Hz), 7.74 (t, 1H, Ar–H, *J* = 8.0 Hz), 7.91 (d, 4H, Ar–H, *J* = 8.8 Hz), 10.64 (s, 1H, NH); ^{13}C NMR (100 MHz) *δ ppm*: 14.66, 61.00, 62.61, 119.18, 125.54, 128.48, 129.75, 130.79, 134.57, 139.66, 142.93, 160.54, 165.67; HRMS (ESI) for $C_{17}H_{18}O_5NS$, calcd 348.09002, found 348.09024 [M+H]$^+$.

4.1.2.9. N-(4-Acetylphenyl)-2-(phenylsulfonyl)acetamide 8c. White crystals, m.p. 209–210 °C, yield 74%, ^{1}H NMR (400 MHz) *δ ppm*: 2.51 (s, 3H, -COC<u>H</u>$_3$), 4.53 (s, 2H, -C<u>H</u>$_2$-CONH-), 7.61 (d, 2H,

Ar−H, J = 8.8 Hz), 7.67 (d, 2H, Ar−H, J = 8.0 Hz), 7.74 (t, 1H, Ar−H, J = 7.6 Hz), 7.91−7.95 (m, 4H, Ar−H), 10.64 (s, 1H, NH); ^{13}C NMR (100 MHz) δ *ppm*: 26.92, 62.66, 119.08, 128.50, 129.75, 130.02, 132.90, 134.58, 139.63, 142.89, 160.54, 197.03; HRMS (ESI) for $C_{16}H_{16}O_4NS$, calcd 318.07946, found 318.07966 $[M+H]^+$.

4.1.2.10. 4-(2-Tosylacetamido)benzoic acid 8d. White crystals, m.p. 255−256 °C, yield 80%, ^{1}H NMR (400 MHz) δ *ppm*: 2.41 (s, 3H, −C_6H_4−CH_3), 4.48 (s, 2H, -CH_2-CO), 7.45 (d, 2H, Ar−H, J = 8.0 Hz), 7.69 (d, 2H, Ar−H, J = 8.8 Hz), 7.78 (d, 2H, Ar−H, J = 8.0 Hz), 7.86 (d, 2H, Ar−H, J = 8.8 Hz), 10.75 (s, 1H, NH D_2O exchangeable), 12.01 (s, 1H, COOH D_2O exchangeable); ^{13}C NMR (100 MHz) δ *ppm*: 21.57, 62.78, 119.33, 128.56, 129.49, 130.19, 134.27, 137.02, 143.14, 145.26, 160.84, 169.25; HRMS (ESI) for $C_{16}H_{16}O_5NS$, calcd 334.07437, found 334.07463 $[M+H]^+$.

4.1.2.11. Ethyl 4-(2-tosylacetamido)benzoate 8e. White crystals, m.p. 187−189 °C, yield 72%, ^{1}H NMR (400 MHz) δ *ppm*: 1.28 (t, 3H, CH_3−CH_2-, J = 7.2 Hz), 2.41 (s, 3H, −C_6H_4−CH_3), 4.26 (q, 2H, CH_3−CH_2-, J = 7.2 Hz), 4.48 (s, 2H, -CH_2-CONH-), 7.45 (d, 2H, Ar−H, J = 8.0 Hz), 7.63 (d, 2H, Ar−H, J = 6.8 Hz), 7.78 (d, 2H, Ar−H, J = 6.8 Hz), 7.92 (d, 4H, Ar−H, J = 6.8 Hz), 10.64 (s, 1H, NH); ^{13}C NMR (100 MHz) δ *ppm*: 21.56, 60.99, 62.76, 119.17, 125.52, 128.53, 130.17, 130.79, 136.86, 142.98, 145.14, 160.61, 165.68; HRMS (ESI) for $C_{18}H_{19}O_5NNaS$, calcd 384.08761, found 384.08751 $[M+Na]^+$.

4.1.2.12. N-(4-Acetylphenyl)-2-tosylacetamide 8f. White crystals, m.p. 216−218 °C, yield 76%, ^{1}H NMR (400 MHz) δ *ppm*: 2.42 (s, 3H, −C_6H_4−CH_3), 2.53 (s, 3H, -COCH_3), 4.47 (s, 2H, -CH_2-CONH-), 7.45 (d, 2H, Ar−H, J = 8.0 Hz), 7.62 (d, 2H, Ar−H, J = 8.8 Hz), 7.78 (d, 2H, Ar−H, J = 8.4 Hz), 7.93 (d, 2H, Ar−H, J = 8.8 Hz), 10.64 (s, 1H, NH D_2O exchangeable); ^{13}C NMR (100 MHz) δ *ppm*: 21.56, 26.91, 62.79, 119.07, 128.54, 130.01, 130.18, 132.88, 136.83, 142.94, 145.16, 160.61, 197.02; HRMS (ESI) for $C_{17}H_{18}O_4NS$, calcd 332.09565, found 332.09521 $[M+H]^+$.

4.1.2.13. N-(4-Nitrophenyl)-2-(phenylsulfonyl)acetamide 10a. Yellow crystals, m.p. 228−230 °C, yield 85%, ^{1}H NMR (400 MHz) δ *ppm*: 4.55 (s, 2H, -CH_2-CONH-), 7.65−7.77 (m, 5H, Ar−H), 7.91 (d, 2H, Ar−H, J = 8.8 Hz), 8.22 (d, 2H, Ar−H, J = 7.6 Hz), 10.92 (s, 1H, NH D_2O exchangeable); ^{13}C NMR (100 MHz) δ *ppm*: 62.69, 119.60, 125.54, 128.52, 129.78, 134.65, 139.52, 143.32, 144.66, 160.97; HRMS (ESI) for $C_{14}H_{12}O_5N_2NaS$, calcd 343.03591, found 343.03600 $[M+Na]^+$.

4.1.2.14. N-(4-Nitrophenyl)-2-tosylacetamide 10b. Yellow crystals, m.p. 235−236 °C, yield 82%, ^{1}H NMR (400 MHz) δ *ppm*: 2.42 (s, 3H, −C_6H_4−CH_3), 4.51 (s, 2H, -CH_2-CONH-), 7.46 (d, 2H, Ar−H, J = 8.0 Hz), 7.74 (d, 2H, Ar−H, J = 9.2 Hz), 7.79 (d, 2H, Ar−H, J = 8.0 Hz), 8.22 (d, 2H, Ar−H, J = 9.2 Hz), 10.91 (s, 1H, NH D_2O exchangeable); ^{13}C NMR (100 MHz) δ *ppm*: 21.57, 62.82, 119.58, 125.54, 125.88, 128.57, 130.21, 136.78, 143.41, 144.67, 145.24, 161.05; HRMS (ESI) for $C_{15}H_{14}O_5N_2NaS$, calcd 357.05156, found 357.05161 $[M+Na]^+$.

4.2. Carbonic anhydrases inhibition

The experimental methodolgy utilized for determination of the CA inhibitory activities for herein prepared target sulfones **(5a-f**, **8a-f** and **10a-b**) were carried out as reported eariler [24−26], and descriped in the Supplementary Materials.

4.3. Anticancer study

Cytotoxicity MTT [27,28], Cell cycle [29,30], and Annexin V-FITC/PI apoptosis [31,32] assays were performed as reported previously, and the detailed procedures were provided in the Supporting Materials.

4.4. Docking

The crystal structures of *h*CA II (PDB 3K34) [33], *h*CA IX (PDB 5FL4) [34] *h*CA XII (PDB 1JD0) [35] were prepared using the Protein Preparation Wizard tool implemented in the Schrödinger suite [36]. The energy minimization protocol with a root mean square deviation (RMSD) value of 0.30 Å was applied using force field OPLS3e. The ligand structures were prepared by Maestro [36b] and evaluated for their ionization states at pH 7.4 ± 0.5 with Epik [36c]. The conjugate gradient method in Macromodel [36e] was used for energy minimization (maximum iteration number: 2500; convergence criterion: 0.05 kcal $mol^{-1}Å^{-1}$). The software Glide was used for docking [36f]. Grids were centered on the centroids of the zinc-coordinating residues and ligands were docked using standard precision mode (SP). The best pose for each compound, evaluated in terms of coordination, hydrogen bond interactions and hydrophobic contacts, was refined by MM-GBSA computations with Prime [36a] using a VSGB solvation model considering the target flexible within 3 Å around the ligand, with this latter distance being considered the best compromise to achieve most reliable binding free energies [37−39].

Funding

The authors extend their appreciation to the Deputyship for Research & Innovation, Ministry of Education in Saudi Arabia for funding this work through the project number "375213500".

Declaration of competing interest

Conflicts of Interest: The authors have declared no conflict of interest.

Acknowledgments

The authors would like to extend their sincere appreciation to the central laboratory at Jouf University for supporting this study. M.M. Al-Sanea also extends his appreciation to the Korea Institute of Science and Technology (KIST) for funding this work through the Grant name “2021 KIST School Partnership Project”.

Appendix A. Supplementary data

Supplementary data to this article can be found online at https://doi.org/10.1016/j.ejmech.2021.113360.

References

[1] C.T. Supuran, Carbonic anhydrases: novel therapeutic applications for inhibitors and activators, Nat. Rev. Drug Discov. 7 (2018) 168−181.
[2] C.T. Supuran, How many carbonic anhydrase inhibition mechanisms exist? J. Enzym. Inhib. Med. Chem. 31 (2016) 345−360.
[3] C.T. Supuran, Structure and function of carbonic anhydrases, Biochem. J. 473 (2016) 2023−2032.
[4] V. Alterio, A. Di Fiore, K. D'Ambrosio, C.T. Supuran, G. De Simone, Multiple binding modes of inhibitors to carbonic anhydrases: how to design specific drugs targeting 15 different isoforms? Chem. Rev. 112 (2012) 4421−4468.
[5] A. Angeli, F. Carta, A. Nocentini, J.Y. Winum, R. Zalubovskis, A. Akdemir, V. Onnis, W.M. Eldehna, C. Capasso, G.D. Simone, S.M. Monti, Carbonic anhydrase inhibitors targeting metabolism and tumor microenvironment, Metabolites 10 (2020) 412.
[6] R.P. Tanpure, B. Ren, T.S. Peat, L.F. Bornaghi, D. Vullo, C.T. Supuran, S.-A. Poulsen, Carbonic anhydrase inhibitors with dual-tail moieties to match the hydrophobic and hydrophilic halves of the carbonic anhydrase active site, J. Med. Chem. 58 (2015) 1494−1501.

[7] Y. Lou, P.C. McDonald, A. Oloumi, S. Chia, C. Ostlund, A. Ahmadi, A. Kyle, U. Auf dem Keller, S. Leung, D. Huntsman, B. Clarke, B.W. Sutherland, D. Waterhouse, M. Bally, C. Roskelley, C.M. Overall, A. Minchinton, F. Pacchiano, F. Carta, A. Scozzafava, N. Touisni, J.Y. Winum, C.T. Supuran, S. Dedhar, Targeting tumor hypoxia: suppression of breast tumor growth and metastasis by novel carbonic anhydrase IX inhibitors, Canc. Res. 71 (2011) 3364–3376.
[8] F. Pacchiano, F. Carta, P.C. McDonald, Y. Lou, D. Vullo, A. Scozzafava, S. Dedhar, C.T. Supuran, Ureido-substituted benzenesulfonamides potently inhibit carbonic anhydrase IX and show antimetastatic activity in a model of breast cancer metastasis, J. Med. Chem. 54 (2011) 1896–1902.
[9] M. Petrenko, A. Güttler, A. Funtan, J. Keßler, D. Emmerich, R. Paschke, D. Vordermark, M. Bache, Combined 3-O-acetylbetulin treatment and carbonic anhydrase IX inhibition results in additive effects on human breast cancer cells, Chem. Biol. Interact. 333 (2020) 109326.
[10] A. Angeli, D. Tanini, T.S. Peat, L. Di C. Mannelli, G. Bartolucci, A. Capperucci, C. Ghelardini, C.T. Supuran, F. Carta, Discovery of new selenoureido analogues of 4-(4-fluorophenylureido) benzenesulfonamide as carbonic anhydrase inhibitors, ACS Med. Chem. Lett. 8 (2017) 963–968.
[11] N. Lolak, S. Akocak, S. Bua, M. Koca, C.T. Supuran, Design and synthesis of novel 1,3-diaryltriazene-substituted sulfonamides as potent and selective carbonic anhydrase II inhibitors, Bioorg. Chem. 77 (2018) 542–547.
[12] S. Akocak, N. Lolak, S. Bua, I. Turel, C.T. Supuran, Synthesis and biological evaluation of novel N,N0-diaryl cyanoguanidines acting as potent and selective carbonic anhydrase II inhibitors, Bioorg. Chem. 77 (2018) 245–251.
[13] W.M. Eldehna, M.F. Abo-Ashour, E. Berrino, D. Vullo, H.A. Ghabbour, S.T. Al-Rashood, G.S. Hassan, H.M. Alkahtani, A.A. Almehizia, A. Alharbi, SLC-0111 enaminone analogues, 3/4-(3-aryl-3-oxopropenyl) amino-benzenesulfonamides, as novel selective subnanomolar inhibitors of the tumor-associated carbonic anhydrase isoform IX, Bioorg. Chem. 83 (2019) 549–558.
[14] M.R. Buemi, A. Di Fiore, L. De Luca, A. Angeli, F. Mancuso, S. Ferro, S.M. Monti, M. Buonanno, E. Russo, G. De Sarro, Exploring structural properties of potent human carbonic anhydrase inhibitors bearing a 4-(cycloalkylamino-1-carbonyl) benzenesulfonamide moiety, Eur. J. Med. Chem. 163 (2019) 443–452.
[15] R.G. Khalifah, The carbon dioxide hydration activity of carbonic anhydrase I. Stop-flow kinetic studies on the native human isoenzymes B and C, J. Biol. Chem. 246 (1971) 2561–2573.
[16] M. Singha, S. Roy, S.D. Pandey, S.S. Bag, P. Bhattacharya, M. Das, A.S. Ghosh, D. Ray, A. Basak, Use of azidonaphthalimide carboxylic acids as fluorescent templates with a built-in photoreactive group and a flexible linker simplifies protein labeling studies: applications in selective tagging of HCAII and penicillin binding proteins, Chem. Commun. 53 (2017) 13015–13018.
[17] R. An, B. Lin, S. Zhao, C. Cao, Y. Wang, X. Cheng, Y. Liu, M. Guo, H. Xu, Y. Wang, Z. Hou, C. Guo, Discovery of novel artemisinin-sulfonamidehybrids as potential carbonicanhydraseIX inhibitors with improved antiproliferative activities, Bioorg. Chem. 104 (2020) 104347.
[18] H. Turkmen, M. Durgun, S. Yilmaztekin, M. Emul, A. Innocenti, D. Vullo, A. Scozzafava, C.T. Supuran, Carbonic anhydrase inhibitors. Novel sulfanilamide/acetazolamide derivatives obtained by the tail approach and their interaction with the cytosolic isozymes I and II, and the tumor-associated isozyme IX, Bioorg. Med. Chem. Lett 15 (2005) 367–372.
[19] W.M. Eldehna, M.F. Abo-Ashour, A. Nocentini, P. Gratteri, I.H. Eissa, M. Fares, O.E. Ismael, H.A. Ghabbour, M.M. Elaasser, H.A. Abdel-Aziz, C.T. Supuran, Novel 4/3-((4-oxo-5- (2-oxoindolin-3-ylidene) thiazolidin-2-ylidene) amino) benzenesulfonamides: synthesis, carbonic anhydrase inhibitory activity, anticancer activity and molecular modelling studies, Eur. J. Med. Chem. 139 (2017) 250–262.
[20] B.J. Henderson, D.J. Carper, T.F. Gonzalez-Cestari, B. Yi, K. Mahasenan, R.E. Pavlovicz, M.L. Dalefield, R.S. Coleman, C. Li, D.B. McKay, Structure-activity relationship studies of sulfonylpiperazine analogues as novel negative allosteric modulators of human neuronal nicotinic receptors, J. Med. Chem. 54 (2011) 8681–8692.
[21] W. Chen, X.-Y. Lu, B.-H. Xu, W.-g. Yu, Z.-n. Zhou, Y. Hu, The rational design and synthesis of water-soluble thiourea ligands for recoverable Pd-catalyzed aerobic aqueous suzuki–miyaura reactions at room temperature, Synthesis 50 (2018) 1499–1510.
[22] H. Xie, D. Ng, S.N. Savinov, B. Dey, P.D. Kwong, R. Wyatt, A.B. Smith 3rd, W.A. Hendrickson, Structure-activity relationships in the binding of chemically derivatized CD4 to gp120 from human immunodeficiency virus, J. Med. Chem. 50 (2007) 4898–4908.
[23] C. Jöst, C. Nitsche, T. Scholz, L. Roux, C.D. Klein, Promiscuity and selectivity in covalent enzyme inhibition: a systematic study of electrophilic fragments, J. Med. Chem. 57 (2014) 7590–7599.
[24] A.A. Alkhaldi, M.M. Al-Sanea, A. Nocentini, W.M. Eldehna, Z.M. Elsayed, A. Bonardi, M.F. Abo-Ashour, A.K. El-Damasy, M.S. Abdel-Maksoud, T. Al-Warhi, P. Gratteri, 3-Methylthiazolo[3,2-*a*]benzimidazole-benzenesulfonamide conjugates as novel carbonic anhydrase inhibitors endowed with anticancer activity: design, synthesis, biological and molecular modeling studies, Eur. J. Med. Chem. 207 (2020) 112745.
[25] W.M. Eldehna, A. Nocentini, Z.M. Elsayed, T. Al-Warhi, N. Aljaeed, O.J. Alotaibi, C.T. Supuran, Benzofuran-based carboxylic acids as carbonic anhydrase inhibitors and antiproliferative agents against breast cancer, ACS Med. Chem. Lett. 11 (2020) 1022–1027.
[26] M.M. Al-Sanea, A. Elkamhawy, S. Paik, S. Bua, S. Ha Lee, M.A. Abdelgawad, C.T. Supuran, Synthesis and biological evaluation of novel 3-(quinolin-4-ylamino) benzenesulfonamides as carbonic anhydrase isoforms I and II inhibitors, J. Enzym. Inhib. Med. Chem. 34 (2019) 1457–1464.
[27] T. Mosmann, Rapid colorimetric assay for cellular growth and survival: application to proliferation and cytotoxicity assays, J. Immunol. Methods 65 (1983) 55–63.
[28] M.A. Said, W.M. Eldehna, A. Nocentini, S.H. Fahim, A. Bonardi, A.A. Elgazar, V. Kryštof, D.H. Soliman, H.A. Abdel-Aziz, P. Gratteri, S.M. Abou-Seri, C.T. Supuran, Sulfonamide-based ring-fused analogues for CAN508 as novel carbonic anhydrase inhibitors endowed with antitumor activity: design, synthesis, and in vitro biological evaluation, Eur. J. Med. Chem. 189 (2020) 112019.
[29] W.M. Eldehna, S.T. Al-Rashood, T. Al-Warhi, R.O. Eskandrani, A. Alharbi, A.M. El Kerdawy,Novel oxindole/benzofuran hybrids as potential dual CDK2/GSK-3β inhibitors targeting breast cancer: design, synthesis, biological evaluation, and in silico studies, J. Enzym. Inhib. Med. Chem. 36 (2021), 270-285.
[30] A. Sabt, W.M. Eldehna, T. Al-Warhi, O.J. Alotaibi, M.M. Elaasser, H. Suliman, H.A. Abdel-Aziz, Discovery of 3, 6-disubstituted pyridazines as a novel class of anticancer agents targeting cyclin-dependent kinase 2: synthesis, biological evaluation and in silico insights, J. Enzyme Inhib. Med. Chem. 35 (2020) 1616–1630.
[31] W.M. Eldehna, G.S. Hassan, S.T. Al-Rashood, T. Al-Warhi, A.E. Altyar, H.M. Alkahtani, A.A. Almehizia, H.A. Abdel-Aziz, Synthesis and in vitro anticancer activity of certain novel 1-(2-methyl-6-arylpyridin-3-yl)-3-phenylureas as apoptosis-inducing agents, J. Enzym. Inhib. Med. Chem. 34 (2019) 322–332.
[32] W.M. Eldehna, A. Nocentini, Z.M. Elsayed, T. Al-Warhi, N. Aljaeed, O.J. Alotaibi, M.M. Al-Sanea, H.A. Abdel-Aziz, C.T. Supuran, Benzofuran-based carboxylic acids as carbonic anhydrase inhibitors and antiproliferative agents against breast cancer, ACS Med. Chem. Lett. 11 (5) (2020) 1022–1027.
[33] C.A. Behnke, I. Le Trong, J.W. Godden, E.A. Merritt, D.C. Teller, J. Bajorath, R.E. Stenkamp, Atomic resolution studies of carbonic anhydrase II, Acta Crystallogr D Biol Crystallogr 66 (2010) 616–627.
[34] J. Leitans, A. Kazaks, A. Balode, J. Ivanova, R. Zalubovskis, C.T. Supuran, K. Tars, Efficient expression and crystallization system of cancer-associated carbonic anhydrase isoform IX, J. Med. Chem. 58 (2015) 9004–9009.
[35] D.A. Whittington, A. Waheed, B. Ulmasov, et al., Crystal structure of the dimeric extracellular domain of human carbonic anhydrase XII, a bitopic membrane protein overexpressed in certain cancer tumor cells, Proc. Natl. Acad. Sci. U.S.A. 98 (2001) 9545–9550.
[36] Schrödinger Suite Release 2020-3, New York, NY, Schrödinger, LLC, vol. 5, 2020, p. 5.(a) Prime.
(b) Maestro v.11.9;.
(c) Epik, v.4.7;.
(d) Impact, v.8.2;.
(e) Macromodel v.12.3.
(f) Glide, v.8.2.
[37] A. Bonardi, A. Nocentini, S. Bua, J. Combs, C. Lomelino, J. Andring, L. Lucarini, S. Sgambellone, E. Masini, R. McKenna, P. Gratteri, C.T. Supuran, Sulfonamide inhibitors of human carbonic anhydrases designed through a three-tails approach: improving ligand/isoform matching and selectivity of action, J. Med. Chem. 63 (2020) 7422–7444.
[38] A. Pustenko, A. Nocentini, P. Gratteri, A. Bonardi, I. Vozny, R. Žalubovskis, C.T. Supuran, The antibiotic furagin and its derivatives are isoform-selective human carbonic anhydrase inhibitors, J. Enzym. Inhib. Med. Chem. 35 (2020) 1011–1020.
[39] A. Bonardi, A. Nocentini, R. Cadoni, S. Del Prete, P. Dumy, C. Capasso, P. Gratteri, C.T. Supuran, J.Y. Winum, Benzoxaboroles: new potent inhibitors of the carbonic anhydrases of the pathogenic bacterium Vibrio cholerae, ACS Med. Chem. Lett. 11 (2020) 2277–2284.